



## Cadmium Removal from aqueous solution by magnetized and polydopamine surface functionalized single-walled carbon nanotubes

SS. Ghasemi<sup>1</sup>, E. Mohammadnia<sup>1</sup>, M. Hadavifar<sup>1\*</sup>, H. Veisi<sup>3</sup>

<sup>1</sup>Graduated Student, Environmental Sciences Department, Hakim Sabzevari University, Sabzevar, Iran

<sup>2</sup>Assistant Professor, Environmental Sciences Department, Hakim Sabzevari University, Sabzevar, Iran

<sup>3</sup>Associate professor, Department of Chemistry, Payame Noor University, Tehran, Iran

### Review History:

Received: 2019-12-05

Revised: 2019-12-16

Accepted: 2019-12-25

Available Online: 2020-01-29

### Keywords:

Magnetic carbon nanotubes

Cadmium

Adsorption kinetics

Isotherm models

Polydopamine

**ABSTRACT:** Pollution of water by heavy metals such as cadmium is becoming a serious ecological and public health hazard due to their toxic effects even at very low concentrations. Thus, the removal of heavy metals from wastewater is very important for controlling environmental pollution. The purpose of this study was removal of cadmium from aqueous solution by polydopamine surface functionalized and magnetized single-walled carbon nanotubes (SWCNTs/Fe<sub>3</sub>O<sub>4</sub>@PDA). In present study, the effects of experimental parameters such as adsorbent dosage, initial metal ion concentration and pH of solution on adsorption Cd (II) in batch system were fully studied. Also, to characterize the adsorbent, SEM and FT-IR analyses were utilized. The results showed that with increasing adsorbent dose and pH the adsorption percentage of cadmium increased and the optimum pH for cadmium removal was determined as pH=7. The results of fitting the data to the isotherm models showed that the Langmuir ( $R^2=0.99$ ), Freundlich ( $R^2=0.97$ ), Temkin ( $R^2=0.97$ ) and Dubinin-Radushkevich ( $R^2=0.96$ ) models logically described the data. The maximum adsorption capacity ( $q_m$ ) was obtained by Langmuir model as 186.48 mg/g which indicates a good absorption capacity of this adsorbent. The obtained experimental adsorption capacity ( $q_e$  exp.) 120.72 mg/g was close to  $q_{e2}$  obtained by pseudo-second-order (PSO) kinetic model (121.95 mg/g). Therefore, it can be concluded that SWCNTs/Fe<sub>3</sub>O<sub>4</sub>@PDA adsorbent can be used as a new adsorbent in optimum conditions for removal of cadmium ions from aqueous solutions.

## 1. INTRODUCTION

One of the most concerning environmental issues in the world is water pollution. Water sources quality gets critical day by day due to rapid industrial development, population increment, the activities of agricultural and other environmental changes [1]. Nonstop discharge of different pollutants such as organic compounds and heavy metals into the environment has led to a serious global concern [2]. Unlike several organic pollutants, heavy metals are non-biodegradable that can accumulate in living tissues. They are also considered as a major threat to human health and the environment [3]. Heavy metals generally include cadmium (Cd), mercury (Hg), arsenic (As), lead (Pb), chromium (Cr), copper (Cu), cobalt (Co), nickel (Ni), zinc (Zn) etc. These ions cause serious adverse health effects [4]. Cd is a heavy metal, which is naturally found in reserves containing other elements. It is highly toxic in a way that it is considered as one of the major contaminations of drinking water [5]. Cd can cause emphysema, kidney damage, hypertension, skeletal abnormalities and cardiovascular disorders even in low concentrations [6]. Regarding these problems,

cadmium removal from wastewater is very important for maintaining community health. Many methods have been employed to remove heavy metals from water; the particular choice is mainly based on the level of initial concentration of heavy metals and economics [5]. Common techniques for removal of metal ions include reverse osmosis, electro-dialysis, resuscitation, oxidation, ion exchange, coagulation-flocculation, membrane filtration, chemical deposition, bioremediation and adsorption [7,8]. However, new technologies are mineral adsorption [9], fluorescent covalent organic framework [10], SO<sub>2</sub> promoted ultrafine nano-sulfur dispersion [11] and magnetic nanomaterial with bifunctional groups and core-shell structure [12]. All of these techniques have their own capabilities and limitations [5]. Among all of the aforementioned methods, surface adsorption is conceded as an effective and economically reasonable technique to treat wastewater. The most significant benefits of surface adsorption compared to other methods are proven as high efficiency, inexpensive and metal recycling possibility. During the past decade, carbon nanotubes (CNTs) were used to eliminate different contaminations from aqueous solutions owing to porous structure, high specific surface area, high interaction and low density with pollutants molecules [13]. Initially,

\*Corresponding author's email: m.hadavifar@hsu.ac.ir, mhadavifar@yahoo.com



CNTs do not interact with some of the materials because of its unique chemical structure; therefore surface modification of CNTs is essential for adsorption of metallic ions [14]. Providentially, chemical surface functionalizing can enhance the distribution of nanotubes in solvents and increase their applicability to the adsorption of aquatic contaminations [15]. Polydopamine is considered as an extremely resistant coating, which is used to coat metals, CNTs, polymers, oxides and magnetic nanoparticles [16]. Polydopamine can bind to heavy metal ions or organic contaminants through covalent and non-covalent interactions such as cutylation, hydrogen bonding,  $\pi$ - $\pi$  interaction and Van der Waals force [17]. Getabi et al. (2016) used magnetic multiwall carbon nanotubes to remove cadmium, efficiently. The results showed that the Freundlich isotherm model was in better agreement with the experimental data than the other isotherms and its maximum adsorption capacity was 81.78 mg/g [18]. In another study, Zhang et al. (2014), used polydopamine biopolymer with magnetic nanoparticles to prepare  $\text{Fe}_3\text{O}_4$ /PDA particles and employed it to eliminate multiple pollutants. Results displayed that under proper pH condition, the highest Langmuir adsorption capacities of 467.3, 112.9, 259.1, 100 and 204.1 mg/g can be attained for pollutants of  $\text{Hg}^{2+}$ ,  $\text{Cu}^{2+}$ ,  $\text{Ag}^+$ , tetrazine and methylene blue, respectively. This indicating great potential of  $\text{Fe}_3\text{O}_4$ /PDA particles for removal of several pollutants [19].

The purpose of the present investigation is to remove Cd (II) ion from aqueous solutions by SWCNTs, which were functionalized by polydopamine. The effect of test parameters such as adsorbent dosage, solution pH, initial metal ion concentration and kinetics were studied, comprehensively.

## 2. MATERIALS AND METHODS

### 2.1. Adsorbent preparation and characterization

At first, 0.5 g of SWCNTs was poured into a container containing 50 ml deionized water under ultrasonic Homogenizer and dispersed for half-hour. Then a 0.45  $\mu\text{m}$  filter paper was used to filter the dispersed CNTs. At that time, CNTs were added to a beaker containing 100 ml 1.5 M NaOH and agitated vigorously. Afterwards, 0.5 g  $\text{FeCl}_2 \cdot 4\text{H}_2\text{O}$  and 1.3 g  $\text{FeCl}_3 \cdot 6\text{H}_2\text{O}$  added to 25 ml deionized water to be dissolved. The solution was then deoxygenized. 0.85 ml concentrated HCl was poured into the solution and it was added to the dispersed CNTs dropwise while being ultra-sonicated. The prepared nanoparticles were separated by a powerful magnet and they were washed three times by 200 ml deionized water. It was dried in an oven at 40 °C that resulted in formation of SWCNT/ $\text{Fe}_3\text{O}_4$ . Finally, 1 g polydopamine was added to 500 ml Tris buffer (10 mM, pH=8.5) containing 1 g SWCNT@ $\text{Fe}_3\text{O}_4$  and stirred for 24 h at ambient temperature. After the reaction (resulting in preparation of SWCNTs/ $\text{Fe}_3\text{O}_4$ @PDA) the prepared particles were collected by a magnet, washed once more with ethanol and deionized water, and dried at room temperature. Fig. 1 demonstrates the functionalization procedure of CNTs. To characterize the functional groups and observe the morphology of the adsorbent, scanning electron microscopy (SEM) and Fourier Transform Infrared (FT-IR)

spectroscopy were utilized, respectively.

### 2.2. Adsorption experiments

The adsorption study of Cd (II) metallic ions from aqueous solutions in the batch system was performed using a 250 mL Erlenmeyer containing 100 mL of metallic ion solution, which was stirred by a magnet stirrer at 200 rpm. Initially, the metallic stock solution was prepared by dissolving Cd (II) salt with the concentration of 1000 mg/L and other required concentrations were prepared daily by diluting the stock solution with deionized water (electrical conductivity=0.05  $\mu\text{S}/\text{m}$ ). To optimize the adsorption process, the effect of adsorbent content was first investigated (100 to 400 mg/L) under constant pH, initial metallic ion concentration at ambient temperature. After determining the optimum amount of adsorbent, adsorption experiments were performed at different pH values (2, 4, 6, 7 and 8). Then, by changing the initial metallic ion concentration (10 to 50 mg/L), the effect of ion concentration was evaluated on the adsorption procedure. During each experiment, samples were taken out after 0, 5, 10, 20, 30, 40, 50 and 60 min of the test initiation. The adsorbent-free metallic ion solution was then transferred into 1.5 mL-plastic vials. After the sampling, the metallic ion concentration in the filtered solution was measured in the range of standard calibration curve. Concentration of the samples containing Cd ions were determined by spectroscopy method using dithizone and UV/VIS spectrophotometer at wavelength of 480 nm [20]. In each experiment, the Cd removal rate and adsorbent efficiency according to maximum adsorption capacity ( $q_e$ ) were determined by Eq. (1) and Eq. (2), respectively.

$$\%R = 100 \times \frac{(C_0 - C_e)}{C_0} \quad (1)$$

$$q_e = \frac{V}{M} (C_0 - C_e) \quad (2)$$

Where,  $C_0$  (mg/L) is the initial concentration Cd (II) in the solution,  $C_e$  (mg/L) is the equilibrium concentration of Cd (II) ions in the solution,  $q_e$  (mg/g) is the mg adsorbed Cd (II) per g adsorbent,  $V$  (L) is working volume and  $M$  (g) is dried weight of the adsorbent.

### 2.3. Adsorption isotherm models

In order to determine the optimum Cd absorption, the consistency of adsorption experimental data with Temkin, Freundlich, Dubinin–Radushkevich and Langmuir isotherm models was evaluated. The Langmuir model is described as Eq. (3) [21].

$$q_e = \frac{q_m b C_e}{1 + b C_e} \quad (3)$$

The Freundlich isotherm is an experimental model. It is based on heterogeneous energy distribution on adsorbent

active sites and multilayer adsorption on heterogeneous surfaces. The Freundlich model is described as Eq. (4) [22].

$$q_e = K_f C_e^{1/n} \quad (4)$$

In equations 3 and 4,  $q_e$  (mg/g) is the adsorption capacity,  $C_e$  (mg/L) is the equilibrium concentration of ions,  $q_m$  (mg/g) is the maximum adsorption capacity of adsorbent and  $b$  (L/mg) is equilibrium constant which is related to bond formation energy during adsorption process. Dubinin-Radushkevich isotherm generally implies the adsorption mechanism with Gaussian energetic distribution on a heterogeneous surface which its nonlinear form is presented as Eq. (5) [20].

$$q_e = q_m \exp(-KE^2) \quad (5)$$

Where,  $E$  is adsorption energy (kJ/mol) that can be calculated by  $E = RT \ln \left( 1 + \frac{1}{C_e} \right)$  or  $E = (2K)^{\frac{1}{2}}$ ,  $K$  (mol/kJ)<sup>2</sup> is Dubinin-Radushkevich isotherm constant,  $R=8.314$  J/mol.K is gas constant and  $T$  (K) is temperature. Temkin adsorption isotherm represents the proportion of the adsorbed material to the logarithm of adsorbing pressure. The linear form of it is expressed as Eq. (6) [23].

$$q_e = B_T \ln K_T + B_T \ln C_e \quad (6)$$

Where,  $B_T$  and  $K_T$  are isotherm constants, which can be attained using the slope and y-intercept of the line drawn by  $q_e$  vs.  $\ln C_e$ .

#### 2.4. Kinetic studies

The pseudo-first-order (PFO) model assumes that the rate of solution adsorption changes directly with time and it is proportional to the changes in the saturation concentration and the rate of adsorption over the time [24]. This model was first proposed by Lagrange as Eq. (7). The Lagrange equation is widely used for adsorption of minerals from aqueous solutions [25].

$$\text{Log}(q_e - q_t) = \text{Log} q_e - \frac{k_1}{2.303} t \quad (7)$$

The PSO kinetic describes the dependence of the rate on the adsorption capacity in the solid phase, which is independent of the concentration of the adsorbing material [26]. This model was expressed by Ho in 1995 as Eq. 8.

$$q_t = \frac{q_e^2 k_2 t}{q_e k_2 t + 1} \quad (8)$$

Where,  $q_e$  (mg/g) and  $q_t$  (mg/g) are the amount of adsorbed material at the time of equilibrium and time  $t$ , respectively.  $k_1$  (1/min) and  $k_2$  (g/mg.min) are reaction rate constants of pseudo-first-order and PSO kinetic models, respectively. Moreover, the initial adsorption rate of  $H$  in terms of mg/g.min is determined via Eq. (9) [27].

$$H = K_2 q_e^2 \quad (9)$$

### 3. RESULTS AND DISCUSSION

#### 3. 1. FTIR spectroscopy analysis

FTIR spectra was used to determine the functional groups in the adsorbent. According to Fig. 1, presence of the peak at 3420  $\text{cm}^{-1}$  was attributed to O-H stretching vibration [28,29].

The breadth and asymmetry of the peak represents the strong hydrogen bonds. These bonds could lead to severe adsorption of water on the surface of the hydrophilic adsorbent [30]. In the spectrum of final synthesized adsorbent, O-H peak was broader than that of raw CNTs. The peaks appeared at 2854  $\text{cm}^{-1}$  and 2920  $\text{cm}^{-1}$  were both assigned to C-H bonding [29]. The peaks observed in the range of 467-630  $\text{cm}^{-1}$  were related to the presence of Fe-O bond that confirm the formation of  $\text{Fe}_3\text{O}_4$  in the prepared adsorbent [20]. The peaks detected at 831  $\text{cm}^{-1}$  [31], 1290  $\text{cm}^{-1}$  [19], 1307  $\text{cm}^{-1}$  [31], 1440 to 1620  $\text{cm}^{-1}$  [32] were assigned to aromatic rings of polydopamine. Furthermore, the peak at 1380  $\text{cm}^{-1}$  was correlated to indole unit of the polydopamine [31]. Consequently, the existence of 1570  $\text{cm}^{-1}$  peak approves the presence of C=C bond [33]. The peak at 1542  $\text{cm}^{-1}$  was assigned to H-N bond. The peak at 1620  $\text{cm}^{-1}$  is a sign of the existence of C=O bond [14]. As

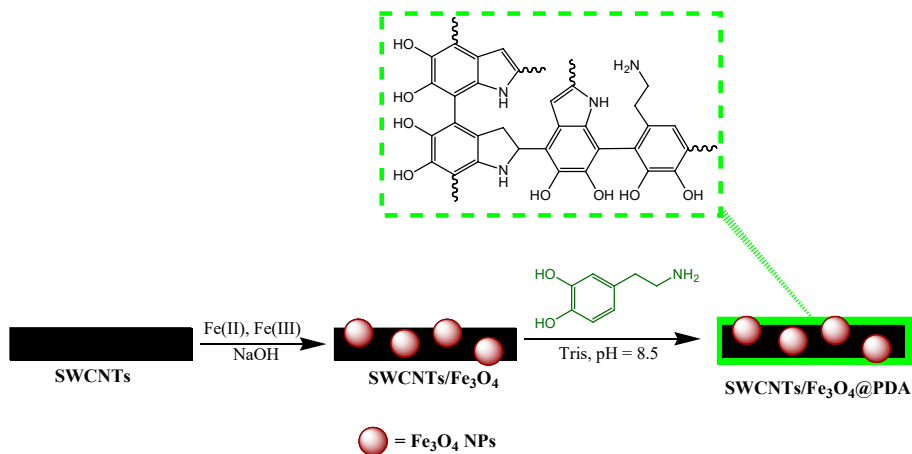


Fig. 1. Schematic of the functionalization of the SWCNTs/Fe<sub>3</sub>O<sub>4</sub>@PDA.

well, the peaks at  $1410\text{ cm}^{-1}$  [34] and  $1035\text{ cm}^{-1}$  were related to C-O stretching vibration [18]. Lastly, the peak at  $1126\text{ cm}^{-1}$  was attributed to C-N stretching vibration [35]. The intensity of the peaks in the FTIR spectra of SWCNTs/ $\text{Fe}_3\text{O}_4$ @PDA was higher than SWCNTs. This confirms the well-functionalized structure of the SWCNTs/ $\text{Fe}_3\text{O}_4$ @PDA adsorbent.

### 3.2. SEM observations

The SEM micrographs of SWCNTs/ $\text{Fe}_3\text{O}_4$ @PDA are illustrated in Fig. 2. As can be seen in the figure there are several bright spots on the functionalized CNTs, which indicates that CNTs were more functionalized on the walls, defect sides and ends [36]. Besides, the functionalized CNTs grew thicker and had a web-like morphology with respect to raw CNTs. This shows the increase of surface area of the functionalized CNTs [37].

### 3.3. The effect of adsorbent dosage on adsorption process

As shown in Fig. 3, with elevating the adsorbent dosage from 100 to 400 mg/L, the rate of cadmium removal increased to 74.13%. The rise in cadmium ion elimination rate can be due to the presence of unsaturated adsorption sites and high specific surface area of the adsorbent [38,39]. On the other

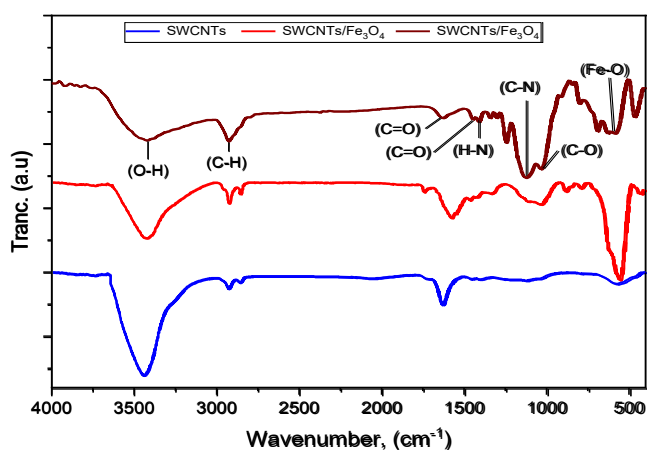


Fig. 2. FTIR spectra of SWCNTs/ $\text{Fe}_3\text{O}_4$ @PDA nanotubes.

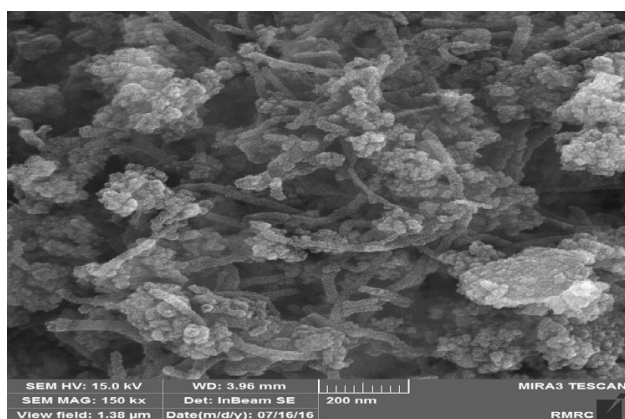


Fig. 3. SEM image of SWCNTs/ $\text{Fe}_3\text{O}_4$ @PDA nanotubes.

side, the equilibrium adsorption capacity reduced because of the unsaturated adsorption sites. SWCNTs/ $\text{Fe}_3\text{O}_4$ @PDA adsorbent effectively eliminated the cadmium ions from the aqueous media due to aromatic ring ligands [40,41]. In a previous investigation by Vukovic et al. (2010), they showed that oxidized carbon nanotubes have more oxygenated groups and perform better in cadmium adsorption. They reported that the oxygenated groups are better proton donors, which results in increase of cation exchange capacity and electrostatic adsorption [42].

### 3.4. The effect of pH on adsorption process

Regarding the Fig. 4, with increasing pH the cadmium removal rate improved from 35.10% at pH=2 to 73.27% at pH=8. By enhancing the pH value, the rate of cation removal increased due to the fact that, at acidic pH values, the presence of  $\text{H}^+$  ions prevents the adsorption of heavy metal ions on the adsorbent surface. Because a competition is occurred between the adsorbent surface and the heavy metal ions to bind with  $\text{H}^+$  ions that prevents the complete adsorption of metallic ions and reduces the removal efficiency [43].

In higher pH values, deprotonation of the adsorbent surface occurs that increases the negative-charged sites. This improves the attraction force between the adsorbent surface and the cations, thus removal efficiency increases [25]. Studies on cadmium described that pH values higher than 6, the predominant type of  $\text{Cd}^{2+}$  is  $\text{Cd}(\text{OH})^+$  [44]. Although, the removal efficiency is high at alkaline or neutral pH values, acidic or neutral pH values were not selected. Since cadmium is present in the form of insoluble hydroxide. This compound either is separated by depositing without adsorbent particles [39], or displays a false removal via depositing on the adsorbent surface [45]. For this reason, the pH of the solutions was considered 7 for all experiments.

### 3.5. The effect of initial metallic ion concentration on the adsorption process

As it is shown in Fig. 5, the highest and the lowest cadmium removal rates were obtained at 10 and 50 mg/L, respectively. Also it can be seen that as the concentration of

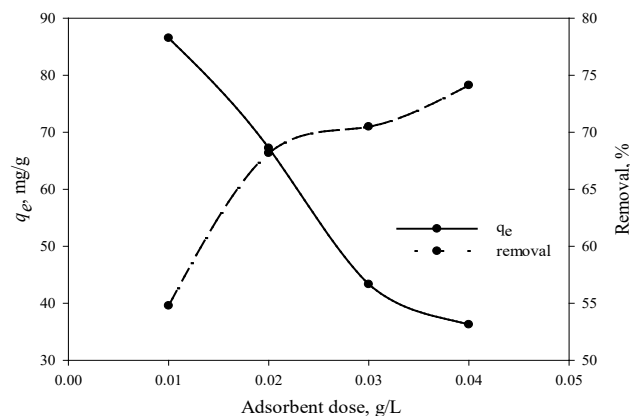
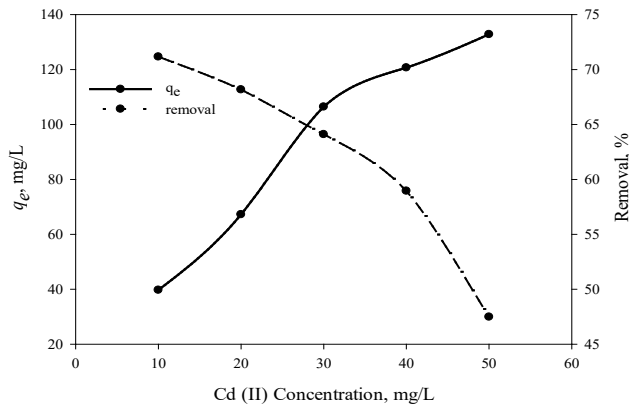
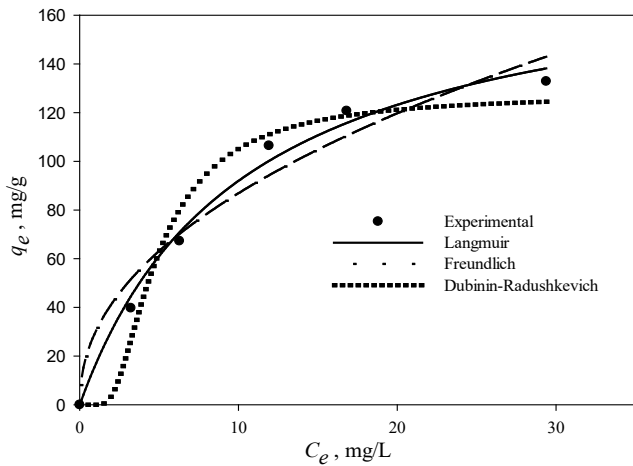


Fig. 4. The effect of adsorbent dose on adsorption percentage and adsorption capacity of cadmium ions under conditions (pH=7, equilibrium time: 60 min and cadmium initial concentration: 20 mg/L).



**Fig. 5. Effect of metal ion concentration on adsorption percentage and adsorption capacity of cadmium ions (adsorbent dosage: 0.2 g/L, equilibrium time 60 min, pH=7).**



**Fig. 6. Adsorption isotherm of Cd(II) on SWCNTs/Fe<sub>3</sub>O<sub>4</sub>@PDA at initial metal ions concentration from 10 to 50 mg/L, adsorbent dose of 0.2 g/L, pH=7 and temperature of 25 °C for 60 min.**

contamination increased, the adsorption capacity improved. In a way that, at the concentration of 10 mg/L, cadmium removal rate and adsorption capacity were 71.16% and 39.73 mg/g, respectively. Conversely, for cadmium concentration of 50 mg/L, the removal rate and adsorption capacity were 47.48% and 132.84 mg/g, respectively.

The increase in adsorption capacity with elevating the pollutant concentration may be due to the improvement of driving force due to the concentration gradient [46]. In addition, the decline in adsorption efficiency by rising the metallic ion concentration could be attributed to the constant number of adsorbent active sites against the increasing number of pollutant molecules. In other words, saturation of the adsorbent surface at high cadmium concentrations was the main cause of this decreasing trend [47]. On the other hand, by increasing the initial concentration of the cadmium ions, a repulsive force between the metallic ions can form that suppresses their adsorption by the adsorbent [48].

### 3.6. Adsorption isotherm models

The adsorption isotherm indicates the relationship between the amount of metal ion adsorbed at constant temperature and its equilibrium concentration in the solution. It also provides essential physicochemical data for evaluation the applicability of the adsorption process as a single operation [30]. The hydrophilic surface of SWCNTs/Fe<sub>3</sub>O<sub>4</sub>@PDA adsorbent leads to an increase in surficial electron density and electronegativity due to the presence of oxygenated functional groups such as carbonyls and aliphatic carboxylic, which plays an important role in the adsorption mechanism [30]. In order to describe the process, four important isotherm models including Langmuir, Freundlich, Dubinin-Radushkevich (nonlinear) and Temkin (linear) were studied. Isotherm studies of cadmium ion removal are demonstrated in Fig. 6. The Temkin model is not shown in the figure because it was in linear form. The experimental data and the fitting coefficients of the adsorption isotherms are presented in Table 1.

Correlation coefficients ( $R^2$ ) of Freundlich, Langmuir, Dubinin-Radushkevich and Temkin models were calculated 0.978, 0.990, 0.962 and 0.975, respectively. However, all models logically describes the adsorption trend, the comparison of correlation coefficients revealed that Langmuir model ( $R^2=0.990$ ) fitted better with the data than other models. The Langmuir model proposes that the adsorption of metal ions occurs as a single layer (or monolayer) on a homogeneous surface [21]. In the Langmuir model, the maximum adsorption capacity ( $q_m$ ) was obtained to be 186.48 mg/g, which is higher than the experimental value of 132.84 mg/g.

### 3.7. Kinetics of the adsorption process

Fig. 7 illustrates the adsorption kinetics of cadmium ions on the SWCNTs/Fe<sub>3</sub>O<sub>4</sub>@PDA adsorbent. Adsorption kinetics control the equilibrium time and affect the adsorption mechanism [49]. The parameters related to these models as well as their correlation coefficients are shown in Table 2.

It is shown that the correlation coefficient of the PFO model for cadmium ions is very low. In contrast, the fitting of

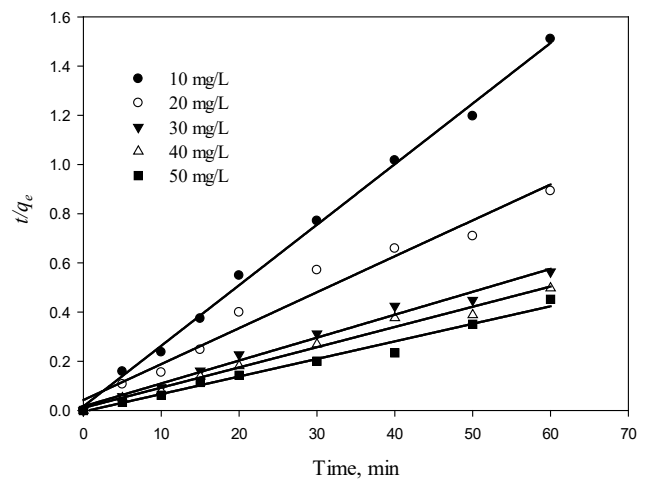


**Fig. 7. PSO of cadmium adsorption onto SWCNTs/Fe<sub>3</sub>O<sub>4</sub>@PDA.**

**Table 1. Freundlich, Langmuir, Temkin and Dubinin–Radushkevich parameters for adsorption of Cd(II) onto SWCNTs/Fe<sub>3</sub>O<sub>4</sub>@PDA.**

Langmuir	$q_m$ , (mg/g)	$b$ , (L/mg)	$R^2$
	186.48	0.0974	0.990
Freundlich	$1/n$	$K_f$	$R^2$
	0.46	30.04	0.978
Dubinin–Radushkevich	$q_m$ , (mg/g)	$E$ (kJ/mol)	$R^2$
	127.51	4.15	0.962
Temkin	$K_T$ (L/mol)	$B_T$	$R^2$
	4.32	3.237	0.975

**Table 2. Kinetic adsorption parameters obtained using PFO model and PSO model.**

Conc. (mg/L)	$q_e(\text{Exp.})$	PFO model			PSO model			
		$K_1$	$q_{e1}$ , (mg/g)	$R^2$	$K_2$	$q_{e2}$ , (mg/g)	$R^2$	$H$
10	39.73	0.106	24.41	0.95	0.035	40.65	0.99	57.83
20	67.23	0.028	19.45	0.14	0.005	68.49	0.97	23.45
30	106.45	0.041	42.07	0.47	0.005	107.52	0.98	61.27
40	120.72	0.043	41.75	0.52	0.006	121.95	0.98	99.64
50	132.84	0.032	48.65	0.32	0.008	140.84	0.98	105.32

the experimental data to the PSO model was good with high correlation coefficient. Therefore, the PSO model reasonably provides a better expression for the experimental data. Low  $k_2$  values in the PSO model also imply that the adsorption process reached equilibrium very rapidly. This indicates that by elevating the metal ion concentration,  $k_2$  values had a general decreasing trend. This also signifies that the active sites of the adsorbent were quickly saturated by cadmium ions, resulting in the formation of monolayer coatings of metallic ions on the adsorbent surface [29,50]. As shown in Table 2, the adsorption rate ( $H$ ) usually increases with enhancing the concentration of adsorbing material in the solution [27].

#### 4. CONCLUSION

The results of this investigation showed that adsorption efficiency increased and the adsorption capacity declined by improving the adsorbent dosage and decreasing the initial metal ion concentration. The prepared adsorbent showed a better efficiency at alkaline pH values for cadmium removal. Comparison of experimental data and fitting coefficients of different adsorption isotherms displayed that the Langmuir model fitted better than other models ( $R^2=0.99$ ). Correlation coefficients ( $R^2$ ) of Freundlich, Langmuir, Dubinin-Radushkevich and Temkin models were calculated 0.978, 0.990, 0.962 and 0.975, respectively. Additionally, analysis of cadmium adsorption kinetics on the adsorbent surface confirmed that the PSO kinetic equation provides good fitting to the experimental data and this model is capable for properly describing the cadmium adsorption mechanism. The  $R^2$  values for PSO model obtained about 0.99 for all metal concentration values. Therefore, it should be stated that, under optimum conditions, single-walled carbon nanotubes functionalized with polydopamine can be used as a novel

adsorbent for elimination of cadmium metallic ions from the aqueous solutions with high efficiency.

#### Compliance with ethical standards

**Competing interests:** Authors declare that they have no competing interests.

#### Funding

This research did not receive any specific grant from funding agencies in the public, commercial, or not-for-profit sectors.

#### ACKNOWLEDGEMENTS

The authors appreciate the financial supporting of the Ministry of Science, Research and Technology of Iran, Hakim Sabzevari University and also, Iran Nanotechnology Initiative Council.

#### REFERENCES

- [1] G. Zeng, X. Li, J. Huang, C. Zhang, C. Zhou, J. Niu, Micellar-enhanced ultrafiltration of cadmium and methylene blue in synthetic wastewater using SDS, J. Hazard. Mater. 185 (2011) 1304–1310. doi:10.1016/j.jhazmat.2010.10.046.
- [2] J. Deng, X. Zhang, G. Zeng, J. Gong, Q. Niu, J. Liang, Simultaneous removal of Cd (II) and ionic dyes from aqueous solution using magnetic graphene oxide nanocomposite as an adsorbent, Chem. Eng. J. 226 (2013) 189–200. doi:10.1016/j.cej.2013.04.045.
- [3] T. Lebeau, D. Bagot, K. Jezequel, B. Fabre, Cadmium biosorption by free and immobilised microorganisms cultivated in a liquid soil extract medium: effects of Cd, pH and techniques of culture, Sci. Total Environ. 291 (2002) 73–83.
- [4] M. Iqbal, A. Saeed, S.I. Zafar, Hybrid biosorbent: an innovative matrix to enhance the biosorption of Cd (II) from aqueous solution, J. Hazard. Mater. 148 (2007) 47–55.
- [5] Ihsanullah, A. Abbas, A.M. Al-Amer, T. Laoui, M.J. Al-Marri, M.S. Nasser, et al., Heavy metal removal from aqueous solution by advanced carbon nanotubes: Critical review of adsorption applications, Sep. Purif.

- Technol. 157 (2016) 141–161. doi:10.1016/j.seppur.2015.11.039.
- [6] H. Qiu, L. Lv, B. Pan, Q. Zhang, W. Zhang, Q. Zhang, Critical review in adsorption kinetic models, *J. Zhejiang Univ. Sci. A*. 10 (2009) 716–724. doi:10.1631/jzus.A0820524.
- [7] T. Liu, Z.-L. Wang, L. Zhao, X. Yang, Enhanced chitosan/Fe<sub>3</sub>O<sub>4</sub>-nanoparticles beads for hexavalent chromium removal from wastewater, *Chem. Eng. J.* 189 (2012) 196–202.
- [8] V.K. Gupta, S. Agarwal, T.A. Saleh, Chromium removal by combining the magnetic properties of iron oxide with adsorption properties of carbon nanotubes, *Water Res.* 45 (2011) 2207–2212. doi:10.1016/j.watres.2011.01.012.
- [9] H. Liu, L. Chang, W. Liu, Z. Xiong, Y. Zhao, J. Zhang, Advances in mercury removal from coal-fired flue gas by mineral adsorbents, *Chem. Eng. J.* 379 (2020) 122263. doi:https://doi.org/10.1016/j.cej.2019.122263.
- [10] Y. He, X. Wang, K. Wang, L. Wang, A triarylamine-based fluorescent covalent organic framework for efficient detection and removal of Mercury(II) ion, *Dye. Pigment.* 173 (2020) 107880. doi:https://doi.org/10.1016/j.dyepig.2019.107880.
- [11] H. Liu, X. Xie, H. Chen, S. Yang, C. Liu, Z. Liu, et al., SO<sub>2</sub> promoted ultrafine nano-sulfur dispersion for efficient and stable removal of gaseous elemental mercury, *Fuel.* 261 (2020) 116367. doi:https://doi.org/10.1016/j.fuel.2019.116367.
- [12] Z. Zhang, K. Xia, Z. Pan, C. Yang, X. Wang, G. Zhang, et al., Removal of mercury by magnetic nanomaterial with bifunctional groups and core-shell structure: Synthesis, characterization and optimization of adsorption parameters, *Appl. Surf. Sci.* 500 (2020) 143970. doi:https://doi.org/10.1016/j.apsusc.2019.143970.
- [13] A. Afkhami, T. Madrakian, A. Amini, Z. Karimi, Effect of the impregnation of carbon cloth with ethylenediaminetetraacetic acid on its adsorption capacity for the adsorption of several metal ions, *J. Hazard. Mater.* 150 (2008) 408–412.
- [14] S.S. Ghasemi, M. Hadavifar, B. Maleki, E. Mohammadnia, Adsorption of mercury ions from synthetic aqueous solution using polydopamine decorated SWCNTs, *J. Water Process Eng.* 32 (2019) 100965. doi:https://doi.org/10.1016/j.jwpe.2019.100965.
- [15] S.H. SHESHMANI, F.M. ARAB, R. AMINI, IRON (III) HYDROXIDE/ GRAPHENE OXIDE NANO COMPOSITE AND INVESTIGATION OF LEAD ADSORPTION, *J. Appl. Res. Chem.* 6 (2013) 17–23.
- [16] J. Liebscher, R. Mrówczyński, H.A. Scheidt, C. Filip, N.D. Hädade, R. Turcu, et al., Structure of polydopamine: a never-ending story?, *Langmuir.* 29 (2013) 10539–10548.
- [17] Z. Zhou, R. Liu, Fe<sub>3</sub>O<sub>4</sub>@polydopamine and derived Fe<sub>3</sub>O<sub>4</sub>@carbon core-shell nanoparticles: Comparison in adsorption for cationic and anionic dyes, *Colloids Surfaces A Physicochem. Eng. Asp.* 522 (2017) 260–265.
- [18] M.P. Gatabi, H.M. Moghaddam, M. Ghorbani, Efficient removal of cadmium using magnetic multiwalled carbon nanotube nanoadsorbents: equilibrium, kinetic, and thermodynamic study, *J. Nanoparticle Res.* 18 (2016) 1–17.
- [19] S. Zhang, Y. Zhang, G. Bi, J. Liu, Z. Wang, Q. Xu, et al., Mussel-inspired polydopamine biopolymer decorated with magnetic nanoparticles for multiple pollutants removal, *J. Hazard. Mater.* 270 (2014) 27–34.
- [20] E. Mohammadnia, M. Hadavifar, H. Veisi, Kinetics and thermodynamics of mercury adsorption onto thiolated graphene oxide nanoparticles, *Polyhedron.* 173 (2019) 114139. doi:https://doi.org/10.1016/j.poly.2019.114139.
- [21] E.D. van Hullebusch, M.H. Zandvoort, P.N.L. Lens, Nickel and cobalt sorption on anaerobic granular sludges: kinetic and equilibrium studies, *J. Chem. Technol. Biotechnol.* 79 (2004) 1219–1227.
- [22] R. Arasteh, M. Masoumi, A.M. Rashidi, L. Moradi, V. Samimi, S.T. Mostafavi, Adsorption of 2-nitrophenol by multi-wall carbon nanotubes from aqueous solutions, *Appl. Surf. Sci.* 256 (2010) 4447–4455.
- [23] A.P. Stafussa, G.M. Maciel, A.G. Da Silva Anthero, M.V. Da Silva, A.A.F. Zielinski, C.W.I. Haminiuk, Biosorption of anthocyanins from grape pomace extracts by waste yeast: kinetic and isotherm studies, *J. Food Eng.* 169 (2016) 53–60. doi:10.1016/j.jfoodeng.2015.08.016.
- [24] M. Taghavi, M.A. Zazouli, Z. Yousefi, B. Akbari-adergani, Kinetic and isotherm modeling of Cd (II) adsorption by L-cysteine functionalized multi-walled carbon nanotubes as adsorbent, *Environ. Monit. Assess.* 187 (2015) 682.
- [25] M. Hadavifar, N. Bahramifar, H. Younesi, M. Rastakhiz, Q. Li, J. Yu, et al., Removal of mercury(II) and cadmium(II) ions from synthetic wastewater by a newly synthesized amino and thiolated multi-walled carbon nanotubes, *J. Taiwan Inst. Chem. Eng.* 0 (2016) 1–9. doi:10.1016/j.jtice.2016.08.029.
- [26] S. Salamat, M. Hadavifar, H. Rezaei, Preparation of nanochitosan-STP from shrimp shell and its application in removing of malachite green from aqueous solutions, *J. Environ. Chem. Eng.* 7 (2019) 103328. doi:https://doi.org/10.1016/j.jece.2019.103328.
- [27] Y.S. Ho, G. Mckay, the Kinetics of Sorption of Divalent Metal Ions Onto Sphagnum Moss Peat, *Water Res.* 34 (2000) 735–742.
- [28] X. Sun, H. Ou, C. Miao, L. Chen, Removal of sudan dyes from aqueous solution by magnetic carbon nanotubes: equilibrium, kinetic and thermodynamic studies, *J. Ind. Eng. Chem.* 22 (2015) 373–377.
- [29] E. Mohammadnia, H. Mojtaba, H. Veisi, Adsorption of Cadmium (II) onto thiolated graphene oxide and kinetic investigations, *Amirkabir J. Civ. Eng.* (2018). doi:10.22060/ceej.2018.14660.5710.
- [30] N.M. Mubarak, J.N. Sahu, E.C. Abdullah, N.S. Jayakumar, Rapid adsorption of toxic Pb (II) ions from aqueous solution using multiwall carbon nanotubes synthesized by microwave chemical vapor deposition technique, *J. Environ. Sci.* 45 (2016) 143–155.
- [31] X. Wang, P.S. Lee, A polydopamine coated polyaniline single wall carbon nanotube composite material as a stable supercapacitor cathode in an organic electrolyte, *J. Mater. Res.* 30 (2015) 3575–3583.
- [32] R. Mrówczyński, R. Turcu, C. Leostean, H.A. Scheidt, J. Liebscher, New versatile polydopamine coated functionalized magnetic nanoparticles, *Mater. Chem. Phys.* 138 (2013) 295–302.
- [33] R. Gao, L. Zhang, Y. Hao, X. Cui, D. Liu, M. Zhang, et al., Novel polydopamine imprinting layers coated magnetic carbon nanotubes for specific separation of lysozyme from egg white, *Talanta.* 144 (2015) 1125–1132.
- [34] S. Saadat, A. Karimi-Jashni, M.M. Doroodmand, Synthesis and characterization of novel single-walled carbon nanotubes-doped walnut shell composite and its adsorption performance for lead in aqueous solutions, *J. Environ. Chem. Eng.* 2 (2014) 2059–2067.
- [35] A.K.S. Deb, V. Dwivedi, K. Dasgupta, S.M. Ali, K.T. Shenoy, Novel amidoamine functionalized multi-walled carbon nanotubes for removal of mercury (II) ions from wastewater: Combined Experimental and density functional theoretical approach, *Chem. Eng. J.* 313 (2017) 899–911.
- [36] Y.Y.-S. Kim, J.J.-H. Cho, S.G. Ansari, H.-I.H. Kim, M.A. Dar, H.-K. Seo, et al., Immobilization of avidin on the functionalized carbon nanotubes, *Synth. Met.* 156 (2006) 938–943. doi:10.1016/j.synthmet.2006.06.003.
- [37] W. Wu, L. Yang, F. Zhao, B. Zeng, A vanillin electrochemical sensor based on molecularly imprinted poly (1-vinyl-3-octylimidazole hexafluoride phosphorus)- multi-walled carbon nanotubes@ polydopamine-carboxyl single-walled carbon nanotubes composite, *Sensors Actuators B Chem.* 239 (2017) 481–487.
- [38] Y.-B. Lin, B. Fugetsu, N. Terui, S. Tanaka, Removal of organic compounds by alginate gel beads with entrapped activated carbon, *J. Hazard. Mater.* 120 (2005) 237–241.
- [39] M.H. Dehghani, M.M. Taher, A.K. Bajpai, B. Heibati, I. Tyagi, M. Asif, et al., Removal of noxious Cr (VI) ions using single-walled carbon nanotubes and multi-walled carbon nanotubes, *Chem. Eng. J.* 279 (2015) 344–352. doi:10.1016/j.cej.2015.04.151.
- [40] C. He-Ying, L. Zhao-Xia, Q. Guo-Li, K. De-Guo, W. Si-Xin, L. Yun-Cai, et al., First-principles study of structures and electronic properties of cadmium sulfide clusters, *Chinese Phys. B.* 17 (2008) 2478–2483. doi:10.1088/1674-1056/17/7/022.
- [41] A. Hutchison, D. Atwood, Q.E. Santillan-jimenez, The removal of mercury from water by open chain ligands containing multiple sulfurs, *J. Hazard. Mater.* 156 (2008) 458–465. doi:10.1016/j.jhazmat.2007.12.042.
- [42] G.D. Vuković, A.D. Marinković, M. Čolić, M.Đ. Ristić, R. Aleksić, A.A. Perić-Grujić, et al., Removal of cadmium from aqueous solutions by oxidized and ethylenediamine-functionalized multi-walled carbon nanotubes, *Chem. Eng. J.* 157 (2010) 238–248. doi:10.1016/j.cej.2009.11.026.
- [43] G. Bhanjana, N. Dilbaghi, K.-H. Kim, S. Kumar, Carbon nanotubes as

- sorbent material for removal of cadmium, J. Mol. Liq. 242 (2017) 966–970. doi:10.1016/j.molliq.2017.07.072.
- [44] M. Sanchez-Polo, J. Rivera-Utrilla, Adsorbent– adsorbate interactions in the adsorption of Cd (II) and Hg (II) on ozonized activated carbons, Environ. Sci. Technol. 36 (2002) 3850–3854.
- [45] M.A. Salam, G. Al-Zhrani, S.A. Kosa, Simultaneous removal of copper (II), lead (II), zinc (II) and cadmium (II) from aqueous solutions by multi-walled carbon nanotubes, Comptes Rendus Chim. 15 (2012) 398–408.
- [46] H. Momenzadeh, A. Khosravi, A.R. Tehrani-Bagha, K. Gharanjig, Investigation of the effective parameters on reactive dye removal from aqueous solution using chitosan nanoparticles emulsion, J. Color. Sci. Tech. 5 (2011) 1–10.
- [47] B. Kakavandi, R.R. Kalantary, A. Esrafiily, A.J. Jafari, A. Azari, Isotherm, kinetic and thermodynamic of Reactive Blue 5 (RB5) dye adsorption using Fe<sub>3</sub>O<sub>4</sub> nanoparticles and activated carbon magnetic composite, J. Color Sci. Technol. 7 (2013) 237–248.
- [48] G. Crini, P.-M. Badot, Application of chitosan, a natural aminopolysaccharide, for dye removal from aqueous solutions by adsorption processes using batch studies: a review of recent literature, Prog. Polym. Sci. 33 (2008) 399–447.
- [49] B. Heibati, M. Ghoochani, A.B. Albadarin, A. Mesdaghinia, A.S.H. Makhlof, M. Asif, et al., Removal of linear alkyl benzene sulfonate from aqueous solutions by functionalized multi-walled carbon nanotubes, J. Mol. Liq. 213 (2016) 339–344.
- [50] M. Hadavifar, N. Bahramifar, H. Younesi, Q. Li, Adsorption of mercury ions from synthetic and real wastewater aqueous solution by functionalized multi-walled carbon nanotube with both amino and thiolated groups, Chem. Eng. J. 237 (2014) 217–228. doi:10.1016/j.cej.2013.10.014.

#### HOW TO CITE THIS ARTICLE

SS. Ghasemi, E. Mohammadnia, M. Hadavifar, H. Veisi, Cadmium Removal from aqueous solution by magnetized and polydopamine surface functionalized single-walled carbon nanotubes, AUT J. Civil Eng., 4(3) (2020) 315-322.

DOI: [10.22060/ajce.2020.17477.5635](https://doi.org/10.22060/ajce.2020.17477.5635)

